PERGAMON

International Journal of Heat and Mass Transfer 44 (2001) 4567–4577

International Journal of HEAT and MASS TRANSFER

www.elsevier.com/locate/ijhmt

Subcooled water critical pressure and critical flow rate in a safety valve

Se Won Kim [a,*], Hee Cheon No [b]

[a] *Reactor & Safety Evaluation Department, Korea Institute of Nuclear Safety, 19 Kusung-dong, Yusubg-gu, Taejon 305-338, Republic of Korea*

[b] *Department of Nuclear Engineering, Korea Advanced Institute of Science and Technology, 371-1 Ku-song Dong, Yu-song Gu, Taejon 305-701, Republic of Korea*

Received 25 February 2001; received in revised form 16 March 2001

Abstract

Subcooled water critical flow phenomena in a safety valve are investigated experimentally at various subcoolings between 10 and 125 K, and about 1 MPa of the inlet pressure with three different disk lifts, 1, 2, and 3 mm. The purpose of this experiment is to find the effects of subcooling and disk lift and to visualize flow patterns in a safety valve when the critical condition is established. All of the experiments show the critical characteristics such as constant throat pressure and constant flow rate when the back pressure is sufficiently decreased. Two correlations, critical pressure ratio and non-equilibrium factor, are developed by using the present experimental data represented in the form of non-dimensional disk lift, subcooling, and pressure. Critical pressure ratios and non-equilibrium factors are considerably affected by different subcoolings while the effect of disk lifts on them is relatively small. A non-equilibrium critical mass flow correlation for the safety valve is also developed based on Fauske's non-equilibrium model and the presented experimental data. The predictions of the correlation are within ±11% of the experimental data. © 2001 Published by Elsevier Science Ltd.

1. Introduction

The systems of nuclear power plants are equipped with many kinds of safety valves. The depressurization rate of the plant system is limited by critical flow rates through the safety valve. Therefore, the predictions of the flow rates through a safety valve are important for the design of industrial high pressure vessels. Safety valves addressed insofar as saturated steam conditions in the safety analyses and the commercial safety valves were usually designed for steam service. However, the real plant data show that the safety relief valves could be under the situation of water or two-phase conditions. Hence, the US NRC specified that the valves should be tested under the full range of expected operating fluid conditions. The physical phenomenon of two-phase choking flow is not well understood when gas and liquid phases are flowing simultaneously through a safety valve.

In the short tube geometry, the experimental critical mass flux of the downstream choking approximated the values predicted by both a surface tension model developed by Burnell [1] and a surface evaporation model proposed by Bailey [2]. Burnell hypothesizes that the surface tension force retards the formation of vapor bubbles, thereby increases the flow rate. Bailey suggested three definite flow regimes. The first regime is related to considerably subcooled condition at all points and the flow curve is represented by the conventional Bernoulli equation. The second regime is associated with metastable flow condition and the flow curve according to the pressure drop shifts suddenly from the first regime to the second one. The third is related to choking flow condition that resembles gaseous critical flow in its effect. Henry and Fauske [3] developed the non-equilibrium homogeneous two-phase

* Corresponding author. Tel.: +82-42-868-0233; fax: +82-42-861-0943.

E-mail address: k119ksw@kins.re.kr (S.W. Kim).

0017-9310/01/$ - see front matter © 2001 Published by Elsevier Science Ltd.
PII: S0017-9310(01)00106-5

Nomenclature

c_f	specific heat of the liquid (J/kg K)
$F(\mathrm{NE})$	non-equilibrium factor
G	mass flux (kg/s m^2)
$\hat{G}$	dimensionless mass flux
h	enthalpy (kJ/kg)
h_{fg}	latent heat of vaporization (kJ/kg)
K_d	valve discharge coefficient
L/D	pipe length to diameter ratio
L^*	disk lift to seat length ratio
P	pressure (MPa)
P^*	outlet pressure to inlet pressure ratio, P_{out}/P_{in}
T	temperature (°C or K)
T^*	subcooling temperature to inlet temperature ratio, T_{sub}/T_{in}
RMSE	root mean square error

Greek symbols

v_{fg}	change in specific volume (m^3/kg)
ρ_f	fluid density (kg/m^3)

Subscripts

b	back
corr	correlation
cr	critical
exp	experiment
in	valve disk inlet condition
o	stagnation inlet condition
out	valve disk outlet condition
sat	saturation
sub	subcooling
t	throat

flow critical model, in which the critical flow rate can be obtained from the energy equation frozen at the inlet quality and it is assumed that the vapor formed is saturated at the local pressure.

In the case of a safety valve, the geometrical and subcooling parameters are very influential on the mass flow rate and on the pressure topology. The thermodynamic non-equilibrium status affected by the geometry is not clear. As the critical condition in a valve strongly depends on the non-equilibrium factors, the observed phenomenon becomes complicated. Several studies have been conducted to clarify the subcooled critical flow in a safety valve and a control valve [4–7]. Their experiments focus on the flow rate and the discharge coefficient of valve. They do not observe the pressure characteristics between the disk and seat surface area (throat or curtain area) because it is not easy to get the data of pressure behavior at the real throat position of the valve.

It can be summarized that there is not only a lack of knowledge regarding the mechanism involved in the flashing of compressed water through a safety valve, but some uncertainty regarding the flow characteristics in a safety valve at such flow situations. Therefore, this research focuses on the visualization of flow patterns, the detection of critical pressure ratios, and the calculation of choked flow rate in a safety valve, including the effect of receiver pressures, disk lifts and subcoolings. With these information it might be possible to more thoroughly understand the critical characteristics of metastability in rapid expansion of two-phase mixture in a safety valve. It might also be possible to contribute to the knowledge needed to establish a more satisfactory flow model indicative of the observed behavior.

2. Thermal non-equilibrium and subcooled flow model

If thermal equilibrium is maintained, liquid flashing occurs as soon as the liquid experiences a pressure lower than its saturation pressure. However, it could be delayed because of the lack of nuclei about which vapor bubbles may form and surface tension which retards their formation, due to heat transfer and other reasons. When the flashing happens, a case of metastability is said to occur. Metastability occurs in rapid expansion, particularly in short flow channels, nozzles and orifices. For sharp edged orifices, the experimental data show that because residence time is short, flashing occurs outside the orifice and no critical pressure exists.

Under the normal condition of flow, the flow rate is proportional to the pressure drop through a valve. However, vapor cavities form when the vena contracta pressure drops below the saturation pressure of liquid with the increase in pressure drop across the valve. Proportionality deteriorates with the vapor formation and flow becomes completely choked when sufficient vapor has formed, so that there may be no increase in flow rate as the valve pressure drop increases. In case of a safety valve, the disk exit pressure is considered to be the throat (vena contracta) pressure and it is the dominant parameter to calculate the flow rate.

Generally, the throat pressure is the unknown variable in a safety valve. Therefore, the valve outlet pressure is used to calculate the flow rate of safety valve. In a safety valve, the flow rate is determined by the Bernoulli equation when the pressures of the inlet and outlet regions are sufficiently high and the fluid is considerably subcooled in both regions:

$$G_{cr\cdot P_{out}} = K_d\sqrt{2\rho_f(P_{in}-P_{out})} \quad \text{for } L/D = 0, \tag{1}$$

where K_d is the valve discharge coefficient (0.61 is recommended for the case of orifice), and ρ_f, P_{in} and P_{out} denote the density of inlet fluid, the inlet pressure and the outlet pressure, respectively. The flow rate calculation of a safety valve is severely affected by the valve coefficient that is given by the valve vender. In a safety valve, the valve coefficient is strongly affected by the disk lifts and by the subcoolings whose effects have not been analyzed systematically.

Fauske [8] performed various experiments on a 0.25 in. inner diameter channels with a sharp edged entrance and the length-to-diameter, L/D, ratios between 0 (an orifice) and 40. The critical pressure ratio was found to be 0.55 for the long channels in which the L/D ratio exceeds 12. For L/D values greater than 0, but less than 12, he recommends to use the following equation:

$$G_{cr\cdot P_{cr}} = K_d\sqrt{2\rho_f(P_o - P_{cr})} \quad \text{for } L/D > 0, \tag{2}$$

where P_{cr} is the throat critical pressure determined by experimental data. If the throat pressure is known, the critical flow rate can be estimated more exactly.

In the absence of significant frictional losses, Fauske [9] proposed the following correlation (considering the non-equilibrium factor in SI units):

$$G_{cr\cdot corr} = \left(\frac{h_{fg}}{v_{fg}}\right)\cdot\sqrt{\frac{1}{F(\mathrm{NE})\cdot T\cdot c_f}}, \tag{3}$$

where $F(\mathrm{NE})$, h_{fg}, v_{fg}, T, and c_f are the non-equilibrium factor, the vaporization enthalpy (kJ/kg), the change in specific volume (m^3/kg), the absolute temperature (K), and specific heat of the liquid (J/kg K), respectively. The non-equilibrium factor is related to many variables such as subcooling, disk lift, and pressure difference between the inlet and outlet of valve. Fauske's non-equilibrium factor correlation mainly depends upon tube length.

Another critical flow correlation considering the subcooling effect was suggested by Fauske. The effect of subcooling on the discharge rate is considered by accounting for the increased single-phase pressure drop $[P_o - P(T_o)]$ resulting from the subcooling, where the subscript o refers to stagnation inlet conditions. The critical flow rate can be stated as

$$G_{cr\cdot Fauske} = \sqrt{2\rho_f K_d^2[P_o - P(T_o)] + G_{cr\cdot corr^2}} \quad \text{for } 0 < L/D < 3, \tag{4}$$

where $G^2_{cr\cdot corr}$ is calculated by Eq. (3) at the inlet pressure $P(T_o)$. $P(T_o)$ denotes the stagnation inlet saturation pressure. If we know the critical pressure and the enthalpy of the water–steam mixture, the critical flow can be calculated by the above four equations. However, there are three unknowns: the critical pressure, the non-equilibrium factor, and the valve discharge coefficient. These values can be determined from experimental data.

3. Experimental apparatus and procedure

The experimental main apparatus consists of a steam generator, a collection tank, nitrogen gas delivery system, and test section. A schematic of the experimental facility and test section is shown in Fig. 1.

These main equipments are connected by 2.5 cm valves and piping. The capacity of the steam generator is 1.3 cubic meters and a 100 kW electric heater is submerged in the tank bottom region. In the test section, the visual windows are installed for the visualization of the flow and void patterns at the inlet and outlet of the valve disk. The disk position of the safety valve can be fixed to any desired lift from 0 to 6 mm using the top mounted micrometer on the test section.

The water temperature in the tank is controlled automatically using the preset temperature switch. The tank pressure is maintained to be constant during the experiment by means of compressed nitrogen and regulating valve. The test line is preheated using the heated water originating from the steam generator.

The flow rate is measured by the hot-water-flow-transmitter that is installed in the horizontal pipe between the steam generator and the test section. The temperatures of the test section are obtained from five temperature transmitters, and the temperatures of the steam generator and the collection tank are also monitored by temperature gages. Seven pressure transmitters are used to get the pressure trends during transient and choking condition. Five pressure transmitters are connected to the test section and two pressure transmitters are connected to the inlet and outlet pipes of the test section. The hole diameter of the pressure and thermocouple taps in the test section is selected as 2 mm to minimize the effect of nucleation in the disk area.

The instrument accuracies of flowmeter, pressure transmitter, and temperature transmitter are $\pm 1\%$, $\pm 0.1\%$, and $\pm 0.1\%$, respectively. The output signal of each variable ranges from 4 to 20 mA. Hence, using the converter with the accuracy of $\pm 0.2\%$, they are changed from 1 to 5 V and recorded to the personnel computer every 1 s. The data acquisition system has the 12 bit resolution for the 5 V and the equivalent error is 0.01 V. The uncertainties of instrumentation are summarized in Table 1.

To analyze the effects of disk lift and subcooling on the critical flow parametrically, the disk inlet pressures are maintained close to 1 MPa (g), subcoolings are between 10 and 125 K, and the disk lifts are selected between 1 and 3 mm. Table 2 shows the test matrix of present experiment.

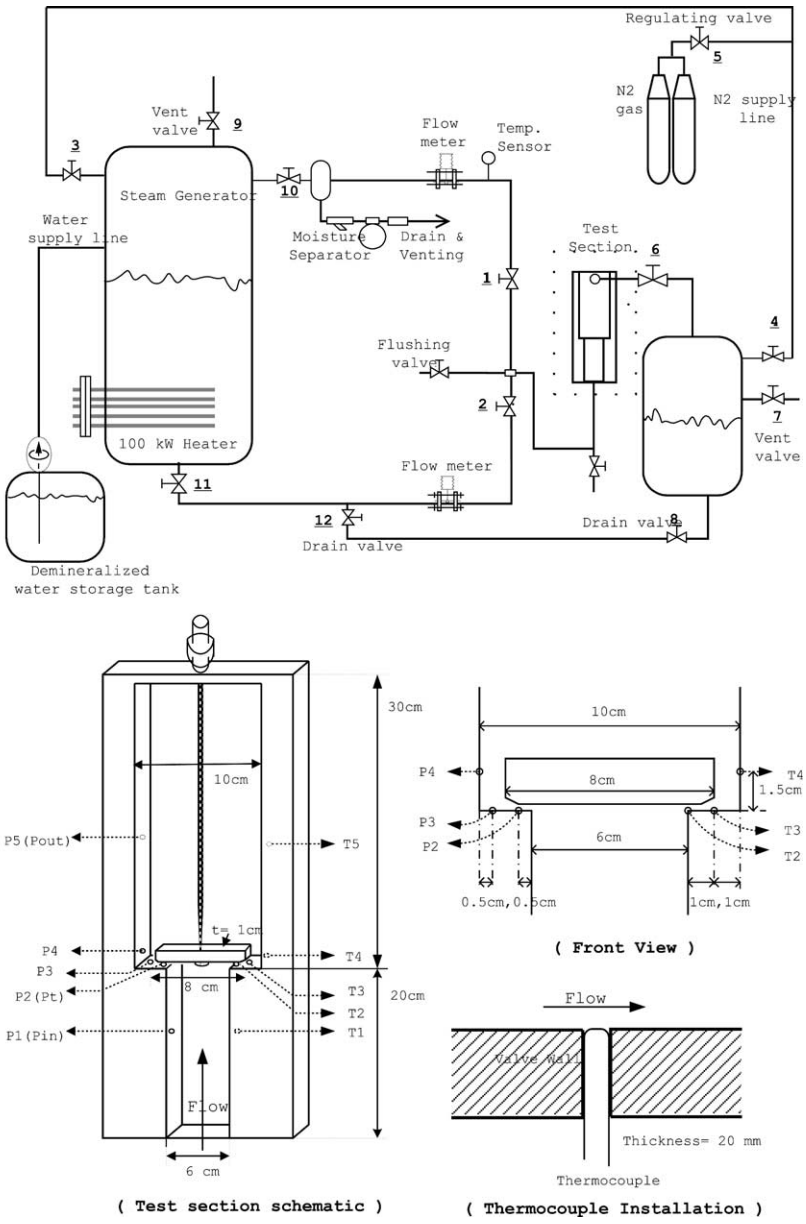

Fig. 1. Schematic drawing of experimental facility and test section.

4. Experimental results and discussion

4.1. General phenomena at the critical state

The test section is designed to observe the flow patterns during the experiment through the visual window.

In the low subcooling water tests, flashing starts at the disk exit and the downstream region of the disk is occupied by steam, when the pressure difference between the inlet and the exit of the disk is large enough.

In the high subcooling water tests, some voids generated just downstream of the disk are seen, even though water at the exit of the disk is still subcooled. The voids collapsed soon in the downstream region and this region is filled with cold water. It is presumed that cavitation may take place due to the strong local circulation flow generated at the disk exit. This may explain why highly subcooled water in the valve tests is choked at a velocity much lower than the liquid-only sonic velocity [10].

Table 1
Data acquisition system and uncertainty of instrumentation

Variable	Range	Gauge accuracy (%)	Type	Computer input signal (V)	Converter error (%)	Total error (%)
Flow rate	0.3–6 m^3/h	1	Vortex	1–5	0.2	1.02
Pressure	0–2 MPa	0.1	Diff.Pres.	1–5	0.2	0.23
Temperature	0–200°C	0.1	K-type	1–5	0.2	0.23

Table 2
Test matrix of present experiment

Test number	Disk lift (mm)	P_{in} (MPa)	T_{in} (°C/K)	T_{sub} (K)
HW01	1	0.975	55/328.15	123.97
HW02	1	1.01	127/400.15	53.32
HW03	1	1.025	141.8/414.95	39.16
HW04	1	1.0	161/434.15	19
HW05	2	0.95	62/335.15	115.67
HW06	2	0.94	125/398.15	52.21
HW07	2	0.98	145/418.15	34.01
HW08	2	1.0	164/437.15	16
HW09	3	0.75	57.5/330.65	110.26
HW10	3	0.85	124.5/397.65	48.44
HW11	3	0.85	145/418.15	27.94
HW12	3	0.875	161/434.15	13.16

As the controlled experimental parameters are the subcooling, disk lift, and pressure drop in the disk region, the phenomena at the critical state are evaluated in this section in terms of the flashing initiation point, the pressure recovery, and the pressure ratio of outlet to inlet of the disk.

4.1.1. Flashing initiation point

When the critical pressure conditions at the throat are established, the flashing initiation locations in the disk region are very important to understand critical flow phenomena. The upstream flashing of the throat takes place when the throat inlet temperature (T2 position in the test section, T_{in}) is greater than the saturation temperature of the throat critical pressure (P2 position in the test section, $T_{sat}(P_{cr})$) even though there is some time retardation due to the surface tension or the lack of nuclei from which vapor bubbles may form. Some superheated liquid in the disk region is converted into saturated vapor. As a result, this flashing of liquid increases the void fraction. Fig. 2 shows the results of $T_{sat}(P_{cr})$ minus T_{in} according to the inlet subcoolings for three disk-lift experiments when the inlet pressures are about 0.8–1 MPa.

In high subcooling water tests, the results of $T_{sat}(P_{cr})$ are always greater than measured T_{in} and flashing does not occur at the P2 position. In low subcooling water tests, the results of $T_{sat}(P_{cr})$ are less than T_{in} and cause the flashing at the P2 position. From Fig. 2, the inlet subcooling effect on the upstream flashing is quite large at high subcooling for 3 mm disk compared to 1 and 2 mm disk lift. This result shows that as the disk lift becomes higher, the location of vena contracta shifts to the upstream of throat and sufficient subcooling is required to prevent the flashing at the upstream of throat. In the present experiment, the required subcoolings for the 1 and 3 mm disk lifts are about 19 and 49 K, respectively.

4.1.2. Pressure recovery

The pressure recovery value in a safety valve is defined as P_{out} minus P_t and it is one of the characteristics to determine choking condition. Fig. 3 shows the two typical experimental results at high and low subcooling.

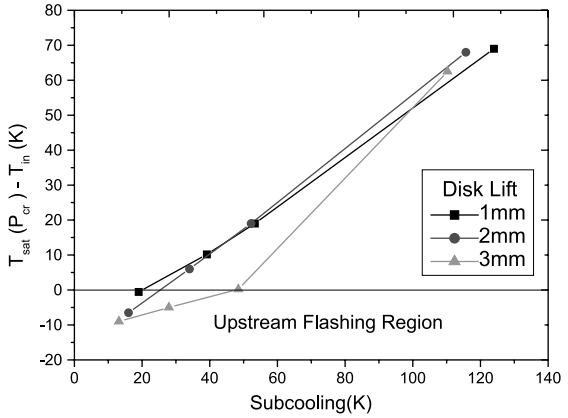

Fig. 2. Effect of subcooling on upstream flashing at different disk lift.

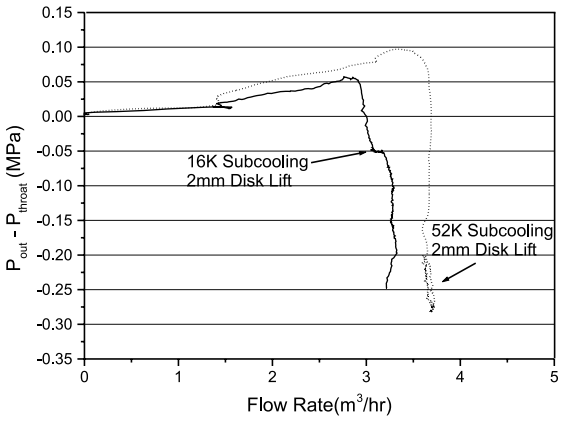

Fig. 3. Flow characteristic for the pressure difference between the disk outlet and the throat.

Before the critical flow condition is established, the outlet pressure is higher than the throat pressure of the disk. After critical flow condition at the throat is established, the outlet pressure becomes smaller than the throat pressure and constant choking flow characteristics come out distinctly. Only one critical flow regime exists in the high subcooling water experiments, while two critical flow regimes exist in the low subcooling water experiments.

4.1.3. Flow trend according to the pressure ratio of P_{out}/P_{in} *and* P_t/P_{in}

Fig. 4 shows the trends of the pressure ratios of P_{out}/P_{in} and P_t/P_{in} for two typical different subcooled water tests.

From Fig. 4, it is evident that the high subcooling water test (test number: HW06) has only one critical

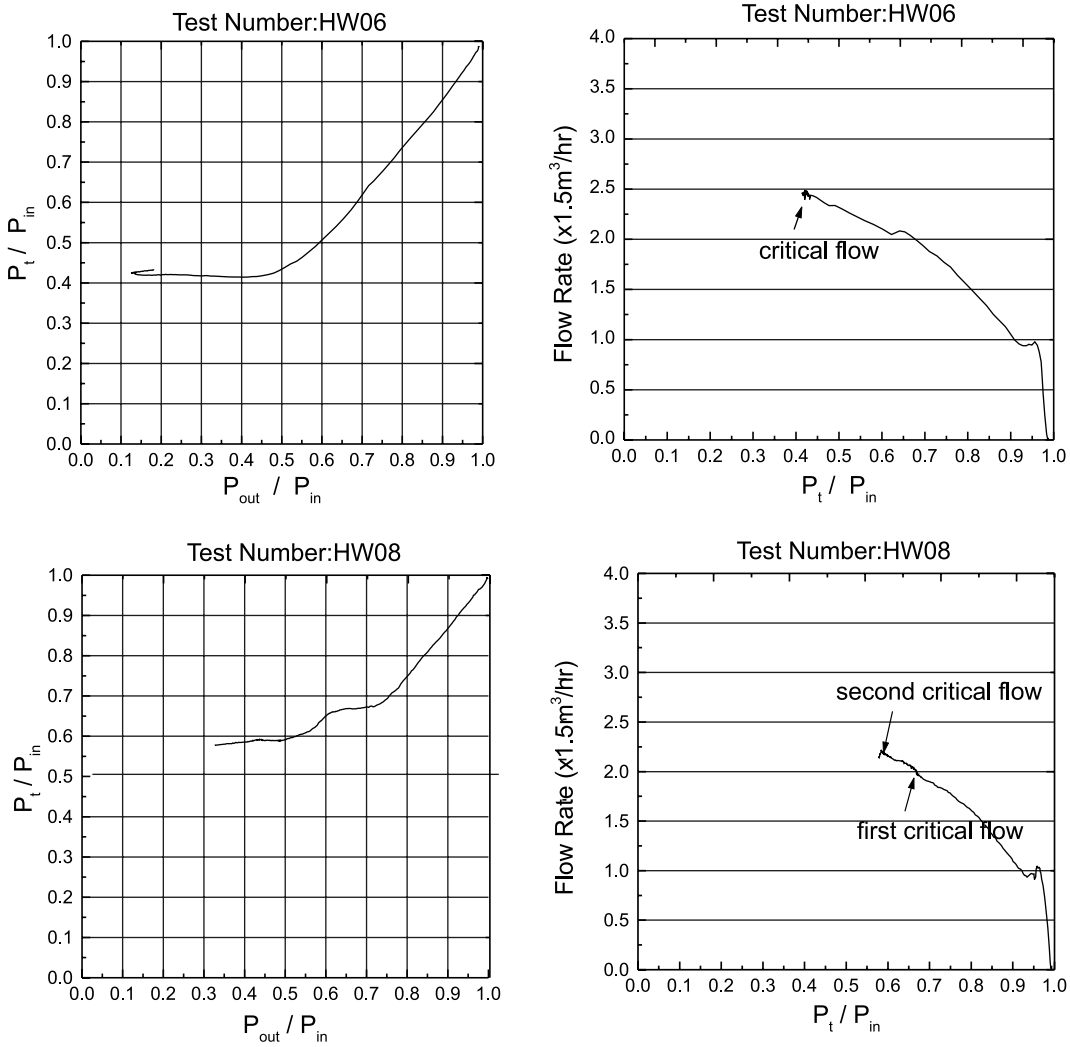

Fig. 4. Characteristics of flow and pressure ratio for cold and hot water (HW06 and HW08).

pressure ratio but the low subcooling water test (test number: HW08) has two critical pressure ratios. For a high subcooled water, one constant throat pressure characteristic exists and the critical flow is not affected by the variation of the back pressure after choking in the same way as that occurred in single-phase flow. For a low subcooled water, two constant throat pressure characteristics exist and the critical flow is affected by the variation of the back pressure after the first choking. Some authors encountered this phenomenon. Zaloudek [11] performed a critical flow test for hot water through tubes shorter than 1.5 in. His experiment showed a four-step flow trend and two constant flow regimes defined as first-step critical and second-step critical. We should consider flashing retardation and downstream void fraction during the critical pressure condition. The first critical throat pressure condition in low subcooled water flow is established by cavitation as in high subcooled water flow with the one constant throat pressure characteristic. Then, as the downstream pressure is decreased

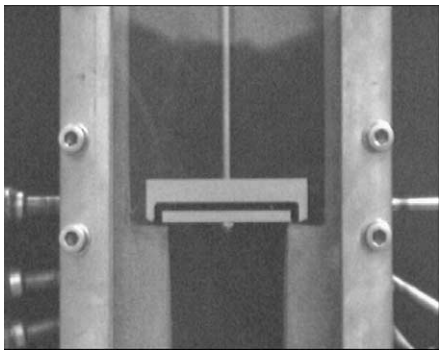

(P_{in} = 0.89, P_t = 0.72, P_{out} = 0.76, MPa)

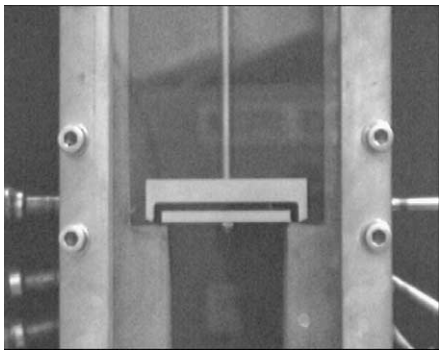

(P_{in} = 0.85, P_t = 0.6, P_{out} = 0.66, MPa)

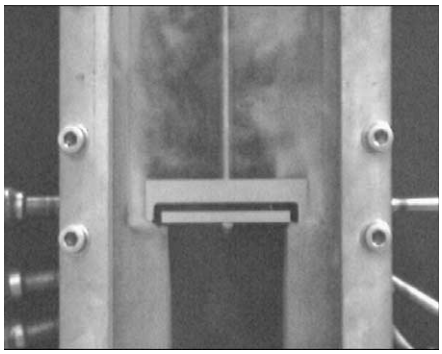

(P_{in} = 0.85, P_t = 0.56, P_{out} = 0.59, MPa)

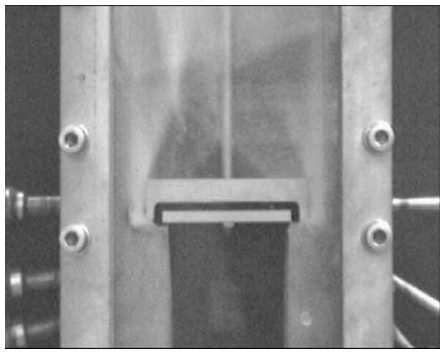

(P_{in} = 0.85, P_t = 0.55, P_{out} = 0.55, MPa)

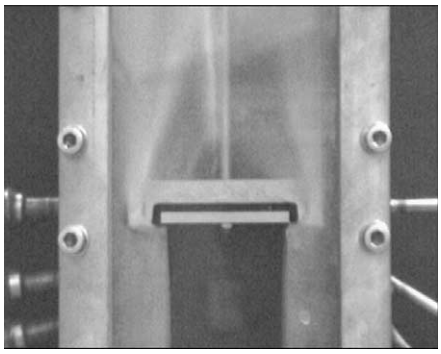

(P_{in} = 0.86, P_t = 0.51, P_{out} = 0.43, MPa)

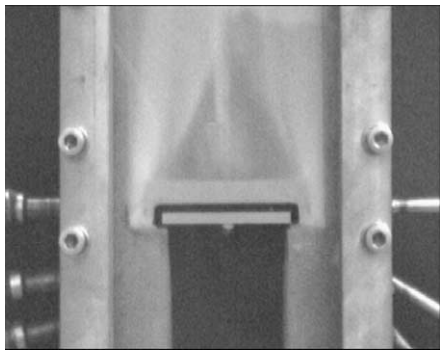

(P_{in} = 0.9, P_t =0.505, P_{out} = 0.26, MPa)

Fig. 5. Typical critical flow patterns for hot water (HW12).

further, cavitation in the downstream section would be decreased due to the perturbation of the flow field resulting from existence of many voids. Therefore, even though the first critical throat pressure condition is established, the critical flow rate is slightly affected by the variation of the back pressure because of an increase in downstream void fraction. Fig. 5 displays void patterns in the low subcooled water test as the back pressure is decreased.

Through the visual observation, the first critical condition occurs when the downstream region of the disk is filled with the subcooled water and the second one does when the same region is filled with the large amount of voids.

4.2. Dimensionless mass flux

In a safety valve, the mass flux of initially compressed water is determined from the relation

$$G = K_d\sqrt{2\rho_{in}(P_{in} - P_{out})}. \tag{5}$$

A dimensionless mass flux is obtained by dividing this equation by $(\rho_{in}\cdot P_{in})^{1/2}$, which gives

$$\hat{G}_{out} = K_d\sqrt{2(1 - P_{out}/P_{in})}. \tag{6}$$

In the real system, the flow is subjected to restriction by the throat pressure thus the dimensionless mass flux is expressed in terms of the throat pressure, P_t, as follows:

$$\hat{G}_t = K_d\sqrt{2(1 - P_t/P_{in})}. \tag{7}$$

Fig. 6 shows two typical high and low subcooling flow trends according to the pressure ratio of P_{out}/P_{in}.

From Fig. 6, it is evident that the measured flow rate is well represented by Eq. (7) and the determined valve coefficients, K_d, are 0.73 and 0.76 for the test number HW06 and HW08, respectively. However, there is a wide discrepancy between the measured flow rate and Eq. (6). Therefore, for the prediction of the flow rate through a safety valve it is better to use the parameter, P_t/P_{in} instead of P_{out}/P_{in}.

4.3. Critical pressure ratio

As explained in Section 4.1, the throat critical pressures come out vividly from high subcooling waters to low subcooling waters as decreasing the back pressure of the test section. The measured critical pressure ratios (P_{cr}/P_{in}) can be defined by a function of valve inlet pressure, inlet temperature, pressure difference of valve in and out, and disk seat length and lift. The non-dimensional expression of these parameters is defined as follows:

$$\begin{aligned} P^* &= P_{out}/P_{in},\\ T^* &= T_{sub}/T_{in},\\ L^* &= \text{Disk lift/Seat length}, \end{aligned} \tag{8}$$

where P_{out} is the disk outlet pressure (0.1–0.3 MPa), P_{in} is the disk inlet pressure (0.85–1 MPa), T_{in} is the valve disk inlet water temperature (323.15–438.15 K), and T_{sub} is the saturation temperature of P_{in} minus T_{in} (10–125 K). The ranges of P^*, T^*, and L^* are 0.10–0.33, 0.03–0.38, and 0.2–0.6, respectively. During the test, the constant throat pressure characteristic exists when the downstream pressure decreases sufficiently. This throat pressure is called the critical pressure (P_{cr}). The critical pressure ratios, P_{cr}/P_{in}, for the variable of T^* and L^* are shown in Fig. 7.

These pressure ratios of high subcooled water ($T^* = 0.4$) and low subcooled water ($T^* = 0.05$) are about 0.25 and 0.6, respectively. They increase as the

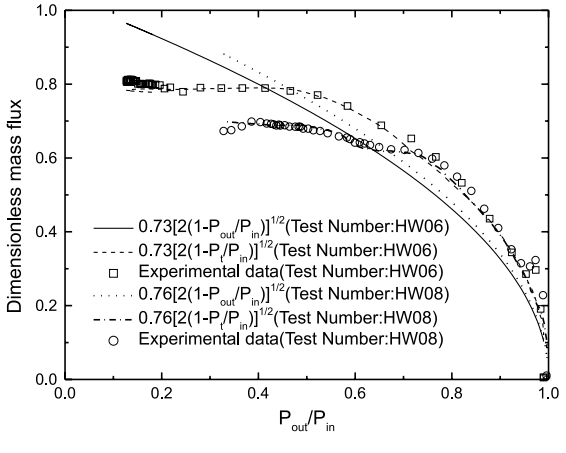

Fig. 6. Experimental and calculated dimensionless flow rate as a function of inlet to outlet pressure ratio (HW06 and HW08).

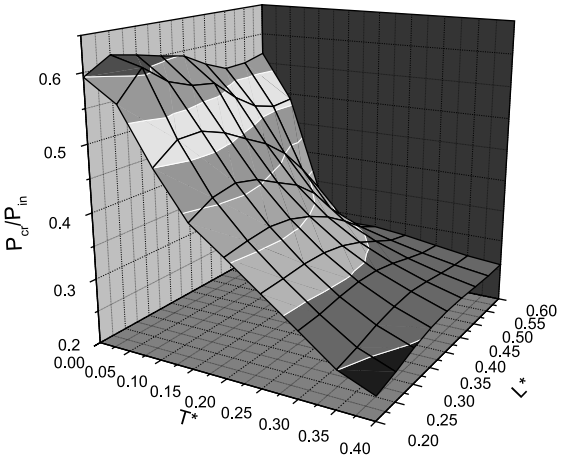

Fig. 7. Variation of critical pressure ratio according to T^* and L^*.

subcoolings or disk lifts decrease. One interesting result of P_{cr}/P_{in} in the low subcooled water ($T^* = 0.05$) test is almost the same as the theoretical critical pressure ratio of wet saturated steam of 0.58 [12]. The critical pressure ratios in the low-lift tests (1 or 2 mm lift) are much higher than those in the high lift (3 mm lift). However, the effect of disk lift on the critical pressure ratio is much smaller than that of subcooling. Using the experimental results, the correlation of the critical pressure ratio is developed as follows:

$$P_{cr}/P_{in} = 0.04828(P^*)^{-0.4605}(T^*)^{-0.5646}(L^*)^{-0.0818} \quad (9)$$

Eq. (9) clearly shows that the critical pressure ratio is highly affected by P^* and T^*, while the effect of L^* on the critical pressure ratio is negligible. Fig. 8 shows the comparison between measured and predicted critical pressure ratios.

There is good agreement between the measured data and the developed correlation with the deviation of +25% and −13%.

4.4. Non-equilibrium factors and critical mass flux

The critical flow rate depends on inlet pressure, outlet pressure, subcooling, and disk lift. The expected mass flow rate is increased with the increase in the inlet pressure and the inlet subcooling. This effect can be explained by the non-equilibrium factor of fluid. Fauske's model, which accounts for non-equilibrium vapor generation by introducing an empirical non-equilibrium coefficient $F(\mathrm{NE})$, is considered here. The constant $F(\mathrm{NE})$ describes the partial phase change at the throat. The critical flow equation, considering the non-equilibrium factor, is described in Eq. (3). The unknown parameter in Eq. (3) is $F(\mathrm{NE})$ and other values are determined by the inlet fluid conditions. Therefore, using the experimental data and Eq. (3), the correlation for the non-equilibrium factor is obtained as follows:

$$F(\mathrm{NE}) = \left(\frac{h_{fg}}{v_{fg}}\right)^2 \cdot \frac{1}{T \cdot c_f} \cdot \frac{1}{(G_{cr\cdot exp})^2}, \quad (10)$$

where $G_{cr\cdot exp}$ is the measured maximum mass flux. Using this equation, the measured non-equilibrium factors in terms of T^* and L^* are calculated.

Fig. 9 shows that the effect of disk lift on the non-equilibrium factor is relatively smaller than that of the subcooling. By using the same non-dimensional parameters, the correlation of the non-equilibrium function $F(\mathrm{NE})$ is expressed as

$$F(\mathrm{NE}) = 0.01519(P^*)^{-0.3186}(T^*)^{-0.5047}(L^*)^{-0.1826}. \quad (11)$$

This correlation is within +14% and −18% of data. Fig. 10 denotes the comparison of the results from the non-equilibrium factor correlation with the measured data.

At the critical state the trends of the critical mass fluxes for T^* and L^* are shown in Fig. 11. From this figure, it is evident that the critical flow rate is also highly dependent on the subcoolings and is slightly dependent on the disk lifts.

From Eqs. (11) and (3), the critical flow correlation considering the non-equilibrium factor can be written as

$$G_{cr\cdot corr} = \frac{h_{fg}(P_{in})}{v_{fg}(P_{in})}\sqrt{\frac{1}{F(\mathrm{NE}) \cdot T(P_{in}) \cdot c_f}}. \quad (12)$$

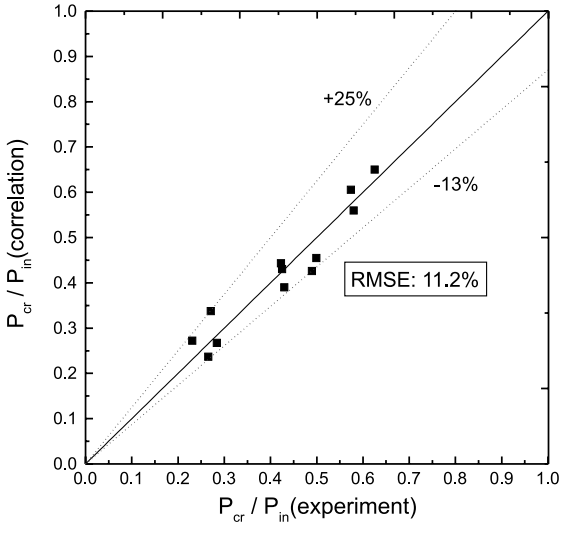

Fig. 8. Comparison between measured and predicted critical pressure ratio.

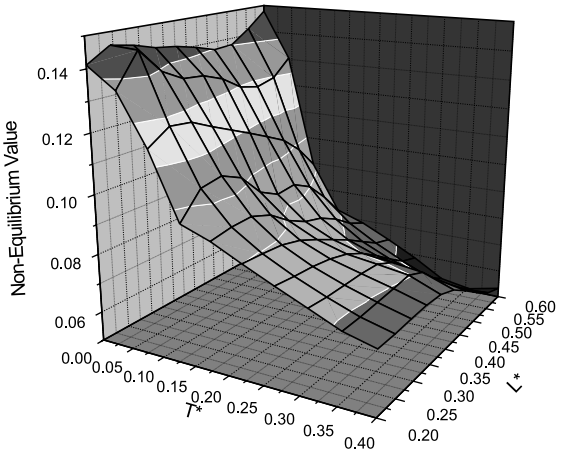

Fig. 9. Variation of non-equilibrium factors according to T^* and L^*.

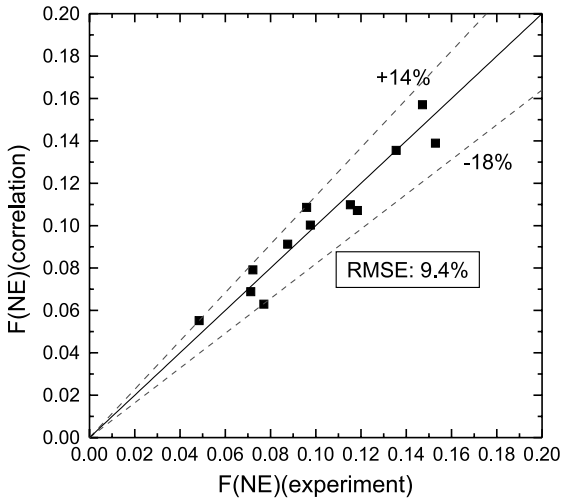

Fig. 10. Comparison between measured and predicted non-equilibrium factor.

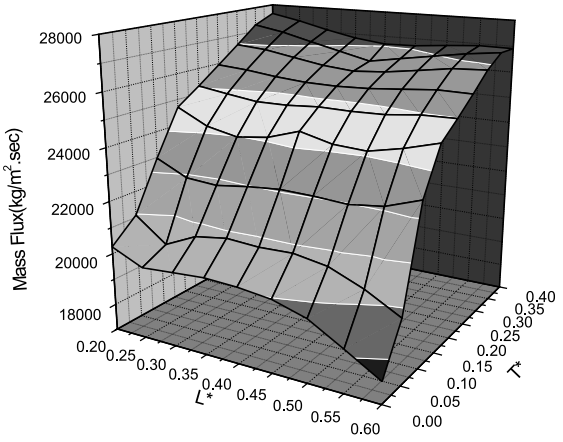

Fig. 11. Variation of critical mass flux according to T^* and L^*.

Considering the hot water test ranges, the variation of specific heat of hot water is from 4.16 to 4.32 kJ/kg K. Therefore, the average value of c_f is set to be approximately 4.2 kJ/kg K. The uncertainty error of c_f is between −1.38% and +0.47%. Calculation results from the present correlation and other correlations such as orifice flow correlations and Fauske's subcooled equation are compared with experimental data in Fig. 12.

In these equations, the valve coefficient, K_d, is 0.61. The orifice flow equation using the back pressure ($G_{cr\cdot P_{out}}$) estimates the critical flow higher than measured values for the low subcooling ranges. The orifice flow equation using the critical pressure value ($G_{cr\cdot P_{cr}}$) gives the smallest values and predicts the critical flow less than experimental data. Fauske's subcooled critical

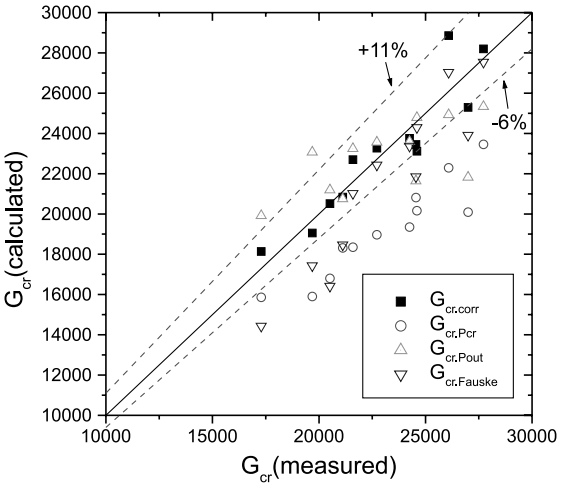

Fig. 12. Comparison of results from several critical flow correlations with measured data.

flow equation ($G_{cr\cdot Fauske}$) shows good agreement with the experimental critical flow data. The predictions of the developed correlation ($G_{cr\cdot corr}$) are within ±11% of data.

5. Conclusions

This study is to provide new experimental results for the critical flow characteristics of subcooled water in a safety valve. The general critical characteristics of subcooled water for the different disk lifts are summarized as follows:

1. It is visually observed that some voids are generated just downstream of the disk even though water at the exit of the disk is still subcooled. This is the clear reason why the highly subcooled water in the valve tests is choked at the velocity much lower than the liquid-only sonic velocity.
2. In the low subcooled water tests, two critical pressure ratios exist while only one critical pressure ratio exists in the high subcooled water tests. In the low subcooled water tests the critical flow rate is slightly affected by the variation of the back pressure because of an increase in downstream void fraction.
3. It turns out that the critical flow rate through the safety valve is mainly governed by flow conditions such as inlet subcooling and inlet pressure while the effect of its geometrical characteristics on the critical flow rate is relatively small.
4. The developed critical flow correlation considering the non-equilibrium factor estimates the critical flow within ±11% of data when the inlet pressures are between 0.85 and 1 MPa, disk lifts between 1 and 3 mm, and subcoolings between 10 and 125 K.

Acknowledgements

The authors gratefully acknowledge financial support from the Korea Institute of Nuclear Safety (KINS).

References

[1] J.G. Burnell, Flow of boiling water through nozzles, orifices and pipes, Engineering 164 (1947) 572–576.
[2] J.F. Bailey, Metastable flow of saturated water, Trans. ASME 73 (1951) 1109–1116.
[3] R.E. Henry, H.K. Fauske, The two-phase critical flow of one-component mixtures in nozzles, orifices, and short tubes, J. Heat Transfer, Trans. ASME (1971) 179–187.
[4] L. Bolle, P. Downar-Zapolski, J. Franco, J.M. Seynhaeve, Experimental and theoretical analysis of flashing water flow through a safety valve, J. Hazardous Mater. 46 (1996) 105–116.
[5] M. Osakabe, M. Isono, Effect of valve lift and disk surface on two-phase critical flow at hot water relief valve, Int. J. Heat Mass Transfer 39 (8) (1996) 1617–1624.
[6] R.E. Henry, R.J. Hammersley, W.E. Berger, B. Deitke, Two-phase critical flow through control valves, ANS Trans. 79 (1998) 340–342.
[7] D. Abdollahian, A. Singh, Prediction of critical flow rates through power-operated relief valves, in: Proceedings or the Second International Topical Meeting on Nuclear Reactor Thermal-Hydraulics, ANS, Santa Barbara, CA, USA, 1982, pp. 912–918.
[8] H.K. Fauske, The discharge of saturated water through tubes, Chem. Eng. Prog. Symp. Ser. 61 (1965) 210.
[9] H.K. Fauske, Flashing flows – some practical guidelines for emergency releases, Plant Oper. Prog. 4 (1985) 132.
[10] E.B. Wylie, V.L. Streeter, Fluid Transients, Feb Press, 1983, p. 7.
[11] F.R. Zaloudek, The critical flow of hot water through short tubes, HW-77594 (1963) 2.
[12] D.W. Sallet, Vapor flow rating of valves using small pressure reservoirs, Nucl. Eng. Des. 72 (1982) 321–327.